Clays and Clay Minerals, Vol. 53, No. 2, 155–161, 2005.

CONVERSION OF CHRYSOTILE TO A MAGNESIAN SMECTITE

MICHAEL CHESHIRE*,† AND NECIP GÜVEN
Texas Tech University, Department of Geosciences, Lubbock, TX 79419, USA

Abstract—Chrysotile from Thetford Mines in Quebec, Canada was treated first with mild formic or oxalic acid at concentrations of 0.5 to 2.0 N at 200ºC in Teflon-lined 12.0 mL Parr bombs. The reaction products were identified by X-ray diffraction as a poorly crystalline Fe-bearing kerolite-like 2:1 layer silicate (which will be described as a kerolitic precipitate or a kerolitic mesophase in this report). Electron microscopic examination showed a thin foily morphology for this kerolitic mesophase that may have formed by the following reaction:

$$\underset{\text{chrysotile}}{Mg_6Si_4O_{10}(OH)_{8(s)}} + 6.02H^+_{(aq)} + 0.54Fe^{2+}_{(aq)} \rightarrow \underset{\text{kerolitic mesophase}}{(Mg_{2.46}Fe^{2+}_{0.54})Si_4O_{10}(OH)_2{\cdot}nH_2O_{(s)}} + 3.55Mg^{2+}_{(aq)} \quad (1)$$

The magnetite impurity in the initial chrysotile asbestos served as the source of Fe in the above reactions. Subsequently, this kerolitic precipitate was reacted with 0.2 N NaOH for 48–96 h at 200ºC and a highly crystalline smectite was formed with the same foily morphology as the kerolitic precipitate. X-ray spectral analyses of the kerolitic mesophase and smectite suggest the following reaction to have taken place:

$$\underset{\text{kerolitic mesophase}}{(Mg_{2.46}Fe^{2+}_{0.54})Si_4O_{10}(OH)_2{\cdot}nH_2O_{(s)}} + 0.53Mg^{2+}_{(aq)} + 0.54NaOH_{(aq)} + 0.01Fe^{3+}_{(aq)} \rightarrow$$
$$\underset{\text{saponite}}{Na_{0.54}(Mg_{2.99}Fe^{2+}_{0.01})(Si_{3.46}Fe^{3+}_{0.54})O_{10}(OH)_{2\,(s)}} + 0.54Si^{4+}_{(aq)} \quad (2)$$

The reaction products, a kerolitic mesophase and smectite, possess a non-fibrous habit in contrast to the fibrous (asbestiform) morphology of chrysotile.

Key Words—Asbestos, Chrysotile, Hydrothermal Conversion, Kerolite, Smectite.

INTRODUCTION

Because of its asbestiform morphology (*i.e.* consisting of long, flexible fibers), chrysotile is considered to be a carcinogenic health hazard in the US and Europe. A comprehensive account of the legal issues and regulations related to asbestos management was presented in 2003 by the Global Environment and Technology Foundation and this report is available on the Internet at the website www.getf.org. Chrysotile is the asbestos widely used in the US and obtained from the Quebec mines in Canada.

The aim of this study is to convert fibrous chrysotile to a hydrous magnesian silicate with a non-hazardous lamellar morphology using mild organic acids. Chrysotile may encounter similar acids during weathering in nature or even in disposal sites like landfills. Chrysotile is a 1:1 trioctahedral phyllosilicate with the chemical formula $Mg_6Si_4O_{10}(OH)_8$ with some Mg substituted by Fe^{2+}. This 1:1 phyllosilicate comprises one Mg octahedral sheet bonded to a Si tetrahedral sheet. An ideal Mg octahedral sheet has a lateral dimension of $b \approx 9.43$ Å and an ideal Si tetrahedral sheet has a lateral dimension of $b \approx 9.1$ Å (Wicks & O'Hanley, 1988). These dimensional differences seem to cause a lateral misfit between the octahedral and tetrahedral sheets along the X and Y directions (Wicks and O'Hanley, 1988; Veblen and Wylie, 1993). To compensate partially for this misfit, the larger octahedral Mg sheet curls over the smaller tetrahedral silica sheet, thus generating chrysotile's tubular morphology. The outer surface of the octahedral magnesian sheet exposes hydroxyl ions (OH^-). Chrysotile's tubular structure produces four reactive sites: (1) an outer hydroxyl sheet; (2) the ends of the fiber; (3) the exposed edges of the curled sheet; and (4) the interior of the hollow central channel (Choi and Smith, 1972; Chowdhury, 1975).

Conversion of chrysotile to a magnesian smectite may involve the removal of one half of the Mg from the chrysotile structure. Vaillancourt (1997) and Barbeau (1979) reported that Mg in chrysotile reacts with acids in two steps: two-thirds of Mg^{2+} is easily leached while the remaining one-third shows resistance to dissolution. We experimented with mild organic acids such as formic acid ($COOH_2$) and oxalic acid ($H_2C_2O_4$) to remove about half of the Mg from the chrysotile structure. Both formic and oxalic acids are abundant in nature, even in some landfill sites where chrysotile can be subjected to weathering by these organic acids. Formic acid is a monoprotic and mild organic acid that decomposes at 200ºC (Bell *et al.*, 1993). The formic acid dissociation equilibrium is represented as the following equation:

$$HCOOH_{(aq)} \rightleftharpoons H^+_{(aq)} + HCOO^-_{(aq)} \qquad (3)$$

---

* E-mail address of corresponding author:
Michael.Cheshire@oildri.com

† Present address: Oil-Dri Corporation of America, 777 Forest Edge Drive, Vernon Hills, IL 60061, USA

DOI: 10.1346/CCMN.2005.0530205

Oxalic acid is a diprotic and moderately strong acid, but decomposes at 175ºC (Kettler *et al.*, 1991). The oxalic acid dissociation equilibrium is represented as the following equations below:

$$H_2C_2O_{4(aq)} \rightleftharpoons H^+{}_{(aq)} + HC_2O_4{}^-{}_{(aq)} \quad (4)$$

$$HC_2O_4{}^-{}_{(aq)} \rightleftharpoons H^+{}_{(aq)} + C_2O_4^{2-}{}_{(aq)} \quad (5)$$

We wanted, first, to establish the optimum concentrations, time and temperature for selectively removing half of the Mg from the chrysotile structure using formic and oxalic acids. We then assessed the effects of temperature, time, ultrasonification, and additives on the recrystallization of smectite in alkaline solutions. Ultrasonification during the crystallization of double-layered hydroxides were shown to increase the crystallite size and crystallinity (Seida *et al.*, 2002). Also, the presence of crystallizing agents, such as NaF and tetramethylammonium chloride (TMaCl), has been reported to enhance the crystallization rate of smectite (Kloprogge *et al.*, 1999).

EXPERIMENTAL PROCEDURES AND METHODS OF ANALYSES

Chrysotile in this study is from the Thetford Mines in Quebec, Canada and was obtained from Ward Geological Supplies (#49-5865). An 88% formic acid solution (Mallinckrodt) and the crystalline form of oxalic acid (Alfa-Aesar) were used to make acidic solutions. The chrysotile samples were first broken up and then cut to ~2–5 mm long with scissors. These cut fibers were then ground in an automated coffee grinder to separate the fibers. These chrysotile fibers were subjected to a series of hydrothermal treatments in 12.0 mL Teflon-lined Parr bombs at 200ºC. First, 0.1 to 0.3 g of chrysotile fibers were pretreated in 12.0 mL of a dilute organic acid (1.0 to 2.0 N) for various periods of time (48–96 h). After acid pretreatment, the intermediate products (precipitates) were centrifuged to remove the remaining acid and Mg in solution. The precipitates were then hydrothermally treated in 12.0 mL of 0.2 N NaOH for 48 to 96 h. The specific experimental conditions are summarized in Tables 1a, 1b, 2a and 2b. After each hydrothermal treatment, reaction vessels were cooled to room temperature (25ºC). Solution pH was measured at 25ºC with a Fisher Accumet® pH Meter, Model 620.

Some samples were subjected to ultrasonification after the acid treatment. Sonification was performed in a Cole Parmer® 4710 series 600 W Ultrasonic Homogenizer for 15 to 60 min, operating at 20 kHz and 10ºC. Following sonification, the intermediate products underwent hydrothermal treatment in 12.0 mL of 0.2 N NaOH. Both the intermediate and final hydrothermal products were examined with X-ray diffraction (XRD) and transmission electron microscopy (TEM).

X-ray diffraction analyses were carried out using a Phillips-Norelco X-ray diffractometer with CuKα-radiation (λ = 0.154184 nm) generated at 40 kV and 25 mA. Samples were smeared on a glass slide and were scanned from 4 to 40º2θ at a rate of 1º2θ/min covering the Bragg angles (θ) from 2 to 20 degrees. Samples were then saturated with ethylene glycol and scanned from 4 to 12º2θ to determine whether any expandable component was present. Patterns were recorded and analyzed using XRD acquisition and processing programs developed by Güven and Subedi (2002) with National Instrument's *LabVIEW* 5.0® programming software. This program presents the XRD pattern as an intensity/θ plot.

The TEM and scanning transmission electron microscopy (STEM) examinations were carried out with a JEOL 100 CX Analytical Electron Microscope operated at 100 kV and 100 µA. The hydrothermal products were

Table. 1 (a) Kerolitic precipitates in reactions of chrysotile in formic acid at 200⁰C.

Sample #	Chrysotile (g)	Formic acid (g)	Pre-pH	Post-pH	Time (h)	Atomic ratios Mg/Si	Atomic ratios Fe/Si	*d* (basal) (nm)
Mao-6	0.1	0.63	2.00	3.98	48	0.602	0.048	0.990
Mao-7, 7r, 24, 52, 56	0.1	1.26	1.91	3.58	48	0.495	0.105	0.991
Mao-57	0.1	1.26	1.91	3.58	48	0.495	0.105	0.991

* Reactants were dispersed in 12.0 mL of deionized water

Table 1. (b) Smectites formed in NaOH treatments of the kerolitic residues (in Table 1a) at 200ºC.

Sample #	NaOH (g)	Pre-pH	Post-pH	Time (h)	Atomic ratios Mg/Si	Atomic ratios Fe/Si	*d* (basal) (nm)
Mao-6	0.10	12.60	12.50	48	0.838	0.072	1.590
Mao-7, 7r, 24, 52, 56	0.10	12.91	12.29	48	0.805	0.116	1.460
Mao-57	0.10	12.91	12.20	72	0.780	0.141	1.520

* Reactants were dispersed in 12.0 mL of deionized water

Table 2. (a) Kerolitic precipitates from oxalic acid treatment of chrysotile at 200^{0}C.

Sample #	Chrysotile (g)	Oxalic acid (g)	Pre-pH	Post-pH	Time (h)	Atomic ratios Mg/Si	Fe/Si	*d* (basal) (nm)
Mao-28	0.1	0.38	1.50	6.38	48	0.582	0.140	0.987
Mao-29	0.1	0.76	1.30	6.03	48	0.570	0.156	1.031
Mao-95	0.1	0.76	1.09	4.27	48	0.590	0.060	1.000
Mao-30	0.1	1.52	1.18	5.90	48	0.524	0.175	0.987

* Reactants were dispersed in 12.0 mL of deionized water

Table 2. (b) Smectites formed in NaOH treatments of the kerolitic residues (in Table 2a) at 200^{0}C.

NaOH (g)	Pre-pH	Post-pH	Time (h)	Atomic ratios Mg/Si	Fe/Si	*d* (basal) (nm)
0.10	13.10	11.08	48	0.874	0.159	1.490
0.10	13.10	12.08	48	0.632	0.160	1.540
0.10	12.87	12.53	48	0.926	0.126	1.500
0.10	13.20	13.30	48	0.696	0.129	1.460

* Reactants were dispersed in 12.0 mL of deionized water

diluted in distilled and deionized water with traces of tertiary butylamine. A drop of this dispersion was dried on a slim bar copper grid coated with a Formvar substrate. The grids were subsequently coated with carbon and platinum. Both TEM and STEM were used to determine the morphology of the reaction products. Energy-dispersive analysis of the X-ray spectra (EDAX) provided the chemical composition of the individual particles. Spectral intensities of the common elements were collected by a KEVEX microanalyzer with a Si(Li) solid-state detector. The spectral intensity ratios were normalized for Si. The Mg/Si and Fe/Si atomic ratios were then calculated by thin-film approximation (Goldstein, 1979). The spectral intensity ratios were converted to atomic ratios by correction factors obtained from a talc standard for Mg/Si ($f_c = 1.47$) and from an annite for Fe/Si ($f_c = 0.73$).

The total amount of Mg^{2+} removed during the acid pretreatment was determined by titration with disodium-ethylenediaminetetraacetic acid (EDTA) as described by Harris (1991). 5 mL of the sample were diluted in 45 mL of deionized (DI) water which was buffered to a pH of 10 with NH_4OH. Six drops of a 0.01% Erichrome Black T were added to the solution as the indicator (red solution). The buffered solution was titrated with a 0.00644/N EDTA solution until equilibrium was reached (blue solution). Each sample was repeated three times and averaged. The results are tabulated in Table 3.

Table 3. Amounts of Mg leached from chrysotile with formic- and oxalic-acid pretreatments at 200 and 100ºC.

	Sample	Chrysotile (g)	Acid concentration	Treatment time (h)	Mg^2 removed (%)
Formic acid 200ºC					
Kerolite crystallized	Mao-104	0.1	2.0 N	96	43
	Mao-105	0.2	2.0 N	96	40
	Mao-106	0.3	2.0 N	96	39
No kerolite crystallized	Mao-102	0.1	2.0 N	72	57
	Mao-103	0.1	2.0 N	96	66
Formic acid 100ºC					
No kerolite crystallized	Mao-77	0.1	2.0 N	6	44
	Mao-73	0.1	2.0 N	12	43
	Mao-72	0.1	2.0 N	24	42
	Mao-71	0.1	2.0 N	36	47
	Mao-70	0.1	2.0 N	48	45
Oxalic acid 200ºC					
Kerolite crystallized	Mao-95	0.1	1.0 N	48	44
	Mao-98	0.1	2.0 N	48	38

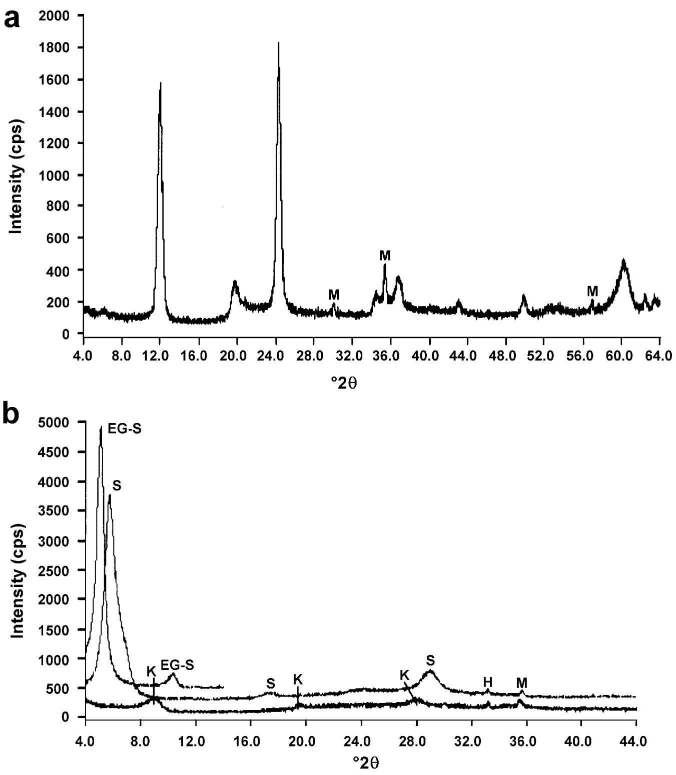

Figure 1. (a) XRD pattern of the starting Thetford clinochrysotile. (b) XRD pattern of the reaction products after hydrothermal treatments of chrysotile with 2.0 N formic acid for 48 h, then with 0.2 N NaOH for 48 h. (K: kerolitic mesophase; S: smectite; EG-S: ethylene glycol treated smectite; H: hematite; M: magnetite).

RESULTS OF INVESTIGATIONS

Thetford chrysotile

The XRD data indicated that the starting material consists of a clinochrysotile ($2Mc_1$) with small impurities of magnetite and brucite (Figure 1a). The concentration of magnetite remained at ~2–5 wt.% throughout the starting material; some hematite was found to precipitate as coatings on magnetite during the hydrothermal reactions. The concentration of brucite varied greatly in the starting materials and those with substantial amounts of brucite were not used in this study. Electron microscopy showed chrysotile with a typical fibrous morphology (asbestiform) with an average fiber diameter of 0.1 μm (Figure 2). The EDAX data indicated a structural formula of $Mg_6Si_4O_{10}(OH)_8$ for the chrysotile with trace amounts of Fe^{2+} in the octahedral positions.

Reaction products of chrysotile upon treatment with formic acid

Chrysotile treated with 2.0 N formic acid for 48 h produced a poorly crystalline kerolitic mesophase, *i.e.* a semicrystalline phase with a few broad and weak basal reflections as shown in in Figure 1b. The average basal spacing of this kerolitic mesophase was 0.993 nm. This kerolitic mesophase (also referred to as a kerolitic precipitate in the following pages) appeared mostly as foils up to 1.0 μm in size and seemed to form as lateral extensions of unfolding chrysotile fibers (Figure 3a,b). Some large aggregates of these kerolitic foils >10 μm in size were also found. These large kerolitic foils had Mg/Si atomic ratios in the range 0.5–0.6 and Fe/Si in the range 0.05–0.11 (Table 1a). The Mg/Si atomic ratios were much lower than expected (0.75) due to X-ray

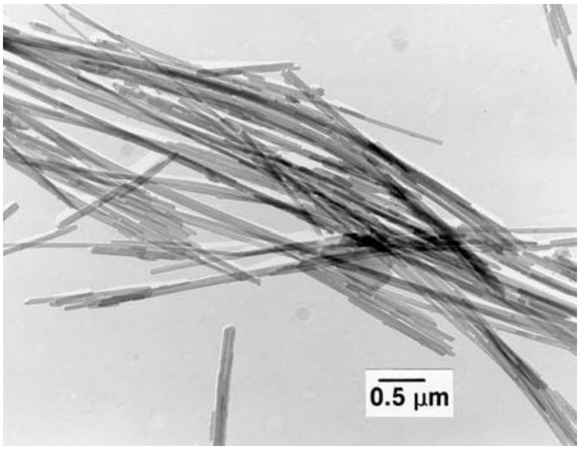

Figure 2. Typical fibrous morphology of Thetford chrysotile (TEM).

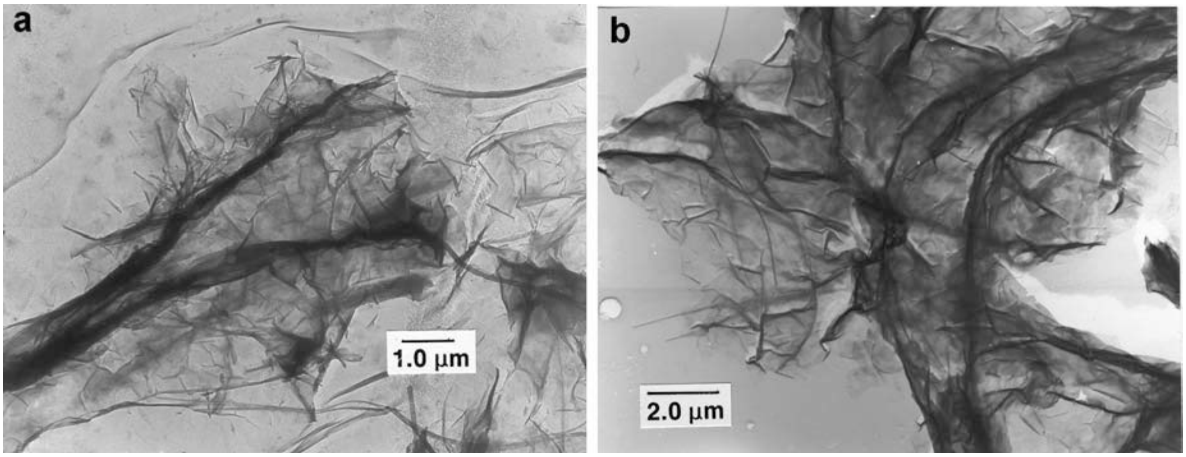

Figure 3. (a) Kerolitic foils forming as extensions or unfolding of chrysotile fibers (TEM). (b) Large kerolitic foils that range from 4 to 40 µm.

amorphous silica that is intimately mixed with these kerolitic foils. Small amounts of hematite were formed from the alteration of magnetite. Some amorphous Mg silicates were also found in the form of globules ranging from 0.03 to 0.10 µm in size. Treating chrysotile with 2.0 N formic acid for 48 h did not consistently yield kerolitic foils. Increasing durations of the acid pretreatments (72 to 96 h), however, did consistently generate kerolitic foils as described above.

Treating 0.2 to 0.3 g of chrysotile with 2.0 N formic acid for 96 h yielded a poorly crystalline kerolitic precipitate with broad XRD reflections and a basal spacing of 0.988 nm. About 10 to 20% of chrysotile survived the hydrothermal reactions. This kerolitic mesophase formed as very large foils up to 40 µm in lateral dimension (Figure 3b) and seemed to extend from the remnant chrysotile fibers. The atomic ratios of the Mg/Si and Fe/Si in these foils were consistent with the other kerolitic foils described above. Buffering the 2.0 N formic acid to a pH of 3.0 (0.21 g Na formate) or decreasing the formic acid concentration to 1.0 N again yielded a poorly crystalline kerolitic mesophase with 10 to 20% chrysotile remaining unreacted.

After hydrothermal treatment with 0.2 N NaOH for 48 h, the above kerolitic precipitate seemed to convert to smectite with no change in the foily morphology. However, XRD patterns indicated that the smectite was highly crystalline in contrast to the poorly crystalline kerolitic precursor. Smectite had an average basal spacing of 1.51 nm that expanded to 1.78 nm upon glycolation (Figure 1b). Smectite foils displayed very similar morphological features to the kerolitic foils (Figure 4a,b). Most of the thin smectite foils extended laterally more than 5 µm and appeared to have significantly higher Mg/Si (0.81) and Fe/Si (0.11) average atomic ratios than those of the kerolitic precursor (Table 1b).

Adding 0.01% NaF and 0.01% TMACl (tetramethylammonium chloride) to the 48 hour alkaline treatment yielded little improvement of the crystallinity of the

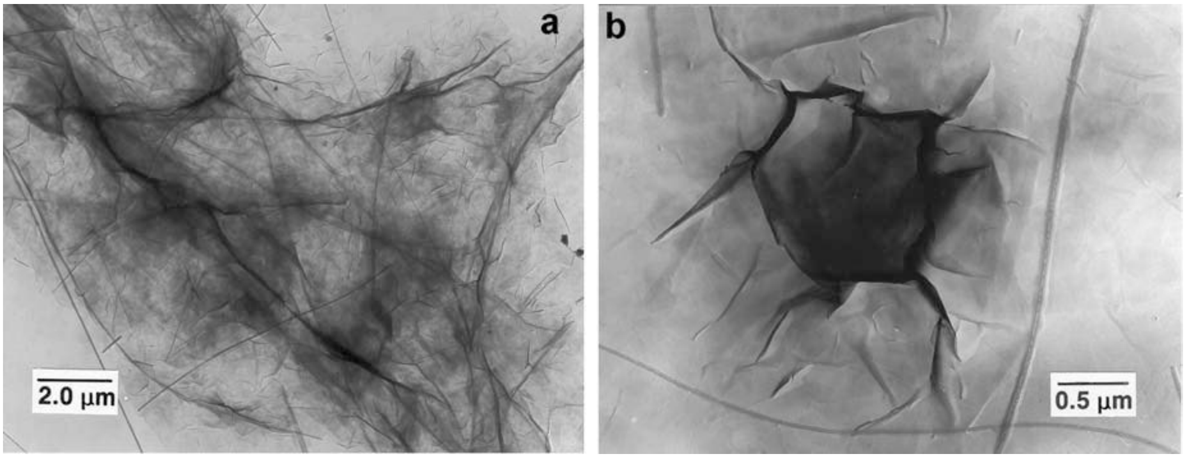

Figure 4. (a) Large smectite foils coalescing to form large mats with residual fibrils of chrysotile (TEM). (b) Small smectite foil with residual fibrils (TEM).

smectite, which again had a basal spacing of 1.51 nm that expanded to 1.71 nm upon glycolation. The smectite foils developed as small individual foils, but often occurred as aggregates >5.0 µm in size. The Mg/Si and Fe/Si atomic ratios did not show any significant changes from the ratios obtained in the smectite foils described above. Small amounts of individual silica fibrils, hematite and small Mg silicates remained throughout the product.

Alkaline reactions over 72 h enhanced the crystallinity of the smectite even in the absence of NaF. Smectite developed a sharp basal reflection of 1.52 nm that expanded to 1.70 nm upon glycolation. Most of the smectite foils have aggregated into large interwoven mats >10 µm in size (Figure 4a). The Mg/Si and Fe/Si atomic ratios did not show any significant change from the ratios obtained in the smectite foils described above. Small X-ray amorphous globules of Mg silicates, hematite and thin X-ray amorphous silica-rich fibrils remained as impurities throughout the final product.

Sonification of the kerolite foils for 15 to 60 min prior to alkaline treatment severely decreased the crystallinity of smectite. Smectite developed broad basal reflections of ~1.30 nm that expanded to 1.67 nm upon glycolation. Sonification increased the concentration of smaller foils extending to no more than 5.0 µm.

Oxalic acid pretreatment of chrysotile fibers

Chrysotile treated with oxalic acid for 48 h at 200ºC generated a poorly crystalline kerolitic precipitate with an average basal spacing of 1.00 nm and average atomic ratios of Mg/Si = 0.56 and Fe/Si = 0.13 (Table 2a). These kerolitic foils crystallized as dense clusters forming long chains with higher Fe content; Fe/Si atomic ratio increased by 0.16 in kerolitic foils.

The kerolitic precipitates treated in alkaline solution at 200ºC with and without 0.01% NaF for 48 h consistently seemed to convert to poorly crystalline smectites with an average basal spacing of 1.49 nm and their Mg/Si and Fe/Si atomic ratios showed wide variations as indicated in Table 2b. Smectite foils developed as dense clusters forming long chains. These clusters have slightly higher Fe content than the precursor kerolite foils.

DISCUSSION OF RESULTS AND CONCLUSIONS

Acid pretreatment

Treatment of chrysotile with formic and oxalic acids seems to generate a Mg/Si ratio in solution favorable for the formation of a kerolitic precipitate (Elton *et al.*, 1997). Dissolution of chrysotile in 2.0 N formic acid for 72 and 96 h consistently yielded a kerolitic precipitate. However, chrysotile treated in oxalic acid for 48 h consistently yielded a morphologically well developed kerolitic phase, regardless of the acid concentration. Differences between the two types of treatment were probably related to the fact that oxalic acid is a stronger acid and stronger chelator than formic acid. However, the oxalate ion undergoes thermal decomposition at 175ºC (Kettler *et al.*, 1991).

Crystallization of these kerolitic foils seemed to start by nucleation on favorable sites exposed by chrysotile fibers. In the formic-acid pretreatments, the edges of the remaining chrysotile fibrils may provide good growth sites for the kerolitic foils because of the similarities between the edge structures of octahedral and tetrahedral sheets of chrysotile and kerolite. In the oxalic-acid pretreatments, chrysotile has mostly been dissolved; therefore, chrysotile tubules do not expose favorable growth sites. Initially, a two-dimensional Mg trioctahedral sheet (with some Fe^{2+} from the partial dissolution of magnetite) probably nucleated. Silica may then condense on both sides of the octahedral sheet, thus forming a kerolite-like 2:1 layer. Crystallization of this kerolitic mesophase continues until silica is depleted from solution, leaving an excess of Mg^{2+}. X-ray spectral data indicate a chemical composition for this kerolitic mesophase to be:

$$(Mg_{2.46}Fe^{2+}_{0.54})Si_4O_{10}(OH)_2{\cdot}nH_2O.$$

The overall reaction of chrysotile to a kerolitic mesophase can then be written as:

$$\underset{\text{chrysotile}}{Mg_6Si_4O_{10}(OH)_{8(s)}} + 6.02H^+_{(aq)} + 0.54Fe^{2+}_{(aq)} \rightarrow \underset{\text{kerolitic mesophase}}{(Mg_{2.46}Fe^{2+}_{0.54})Si_4O_{10}(OH)_2{\cdot}nH_2O_{(s)}} + 3.55Mg^{2+}_{(aq)} \quad (6)$$

Alkaline treatment of a kerolitic precipitate

In alkaline solutions, a kerolite was reported to undergo a solid-state transformation to a trioctahedral Mg-smectite (Pozo & Casas, 1999; Elton *et al.*, 1997). The similar foily morphologies of this kerolitic mesophase and smectite in our study suggest a topotactic conversion of the former to smectite. X-ray spectral data suggest the smectite product has a chemistry similar to an Fe-bearing saponite:

$$Na_{0.54}(Mg_{2.99}Fe^{2+}_{0.01})(Si_{3.46}Fe^{3+}_{0.54})O_{10}(OH)_2$$

The Fe^{2+} in the octahedral position of this kerolitic mesophase seems to be oxidized to Fe^{3+} and to replace Si^{4+} in the tetrahedral sheets. The vacant Fe positions in the octahedral sheets seem to be filled with Mg^{2+}. Thus, the conversion of the kerolitic phase to an Fe-bearing saponite can be represented by the reaction:

$$\underset{\text{kerolitic phase}}{(Mg_{2.46}Fe^{2+}_{0.54})Si_4O_{10}(OH)_2{\cdot}nH_2O_{(s)}} + 0.53Mg^{2+}_{(aq)} + 0.54NaOH_{(aq)} + 0.01Fe^{3+}_{(aq)} \rightarrow \underset{\text{saponite}}{Na_{0.54}(Mg_{2.99}Fe^{2+}_{0.01})(Si_{3.46}Fe^{3+}_{0.54})O_{10}(OH)_{2\,(s)}} + 0.54Si^{4+}_{(aq)} \quad (7)$$

A −1.07 charge imbalance in the kerolitic phase to saponite reaction develops because magnetite, the likely oxidizing agent, is not included in the reaction.

In conclusion, fibrous chrysotile can be converted in mild organic acids at 200ºC to a kerolite-type layer silicate with a foily morphology. Further treatment of this kerolitic phase with alkaline solutions can transform the kerolitic phase to a smectite with thin foil morphology. Such conversion of chrysotile to a kerolite or smectite can also occur in nature where organic acids react with chrysotile.

ACKNOWLEDGMENTS

We sincerely appreciate the reviews of the manuscript by J.T. Kloprogge and Peter Heaney. Their criticisms and suggestions significantly improved the presentation of this paper. We would also like to thank Dr Dominick Casadonte and Dr Zhengrong Li from Texas Tech's Chemistry Department for their assistance with the sonification reactions.

REFERENCES

Barbeau, C. (1979) Evaluation of chrysotile by chemical methods. Pp. 197–212 in: *Mineralogical Techniques of Asbestos Determination* (R.L. Ledoux, editor). Short Course Handbook **4**. Mineralogical Association of Canada, Toronto, Canada.

Bell, J.L., Wesolowski, D.J. and Palmer, D.A. (1993) The dissociation quotients of formic acid in sodium chloride solutions to 200ºC. *Journal of Solution Chemistry*, **22**, 125–136.

Choi, I. and Smith, R.W. (1972) Kinetic study of dissolution of asbestos fibers in water. *Journal of Colloid and Interface Science*, **40**, 253–262.

Chowdhury, S. (1975) Kinetics of leaching of asbestos minerals at body temperature. *Journal of Applied Chemical and Biotechnology*, **25**, 347–353.

Elton, N.J., Hooper, J.J. and Holyer, V.A.D. (1997) An occurrence of stevensite and kerolite in the Devonian Crousa gabbro at Dean Quarry, The Lizard, Cornwall, England. *Clay Minerals*, **32**, 241–252.

Goldstein, J.I. (1979) Principles of thin film X-ray microanalysis. Pp. 83–120 in: *Introduction to Analytical Electron Microscopy* (J.T. Hren, J.I. Goldstein and D.C. Joy, editors). Plenum Press, New York and London.

Güven, N. and Subedi, R. (2002) *Using a PC-based LabVIEW Program for Acquiring and Processing X-Ray Diffraction Data*. www.ni.com/pdf/csma/us/necip_guven.pdf

Harris, D.C. (1991) *Quantitative Chemical Analysis*, 3rd edition. W.H. Freeman and Company, New York, 782 pp.

Kettler, R.M., Palmer, D.A. and Wesolowski, D.J. (1991) Dissociation quotients of oxalic acid in aqueous sodium chloride media to 175ºC. *Journal of Solution Chemistry*, **20**, 905–926.

Kloprogge, J.T., Komarneni, S. and Amonette, J. (1999) Synthesis of smectite clay minerals: a critical review. *Clay and Clay Minerals*, **47**, 529–554.

Pozo, M. and Casas, J. (1999) Origin of kerolite and associated Mg clays in palustrine-lacustrine environments. The Esquivias deposit (Neogene Madrid Basin, Spain). *Clay Minerals*, **34**, 395–418.

Seida, Y., Nakano, Y. and Nakamura, Y. (2002) Crystallization of layered double hydroxides by ultrasound and the effects of crystal quality on their surface properties. *Clays and Clay Minerals*, **50**, 525–532.

Vaillancourt, A., Denes, G. and Le Van Mao, R. (1997) Reactivity of chrysotile asbestos in acids: mechanisms of transformation to silicon dioxide hemihydrate upon leaching of magnesium. *Materials Research Society Symposium Proceedings*, **453**, 71–76.

Veblen, D.R. and Wylie, A.G. (1993) Mineralogy of amphiboles and 1:1 layer silicates. Pp. 61–137 in: *Health Effects of Mineral Dusts* (G.D. Guthrie and B.T. Mossman, editors). Reviews in Mineralogy, **28**. Mineralogical Society of America, Washington, D.C.

Wicks, F.J. and O'Hanley, D.S. (1988) Serpentine minerals: structure and petrology. Pp. 91–159 in: *Hydrous Phyllosilicates* (S.W. Bailey, editor). Reviews in Mineralogy, **19**. Mineralogical Society of America, Washington, D.C.

(*Received 20 January 2004; revised 12 November 2004; Ms. 875; A.E. Peter J. Heaney*)